THE DIURNAL VARIATION AND RADIATIVE INFLUENCE OF MARTIAN WATER ICE CLOUDS

R. J. Wilson , *Geophysical Fluid Dynamics Laboratory, Princeton, NJ (John.Wilson@noaa.gov),* **M. D. Smith, and G. Neumann**, *NASA Goddard Space Flight Center, Greenbelt, MD., USA.*

Introduction: The aphelion season is characterized by the presence of a prominent tropical water ice cloud belt [*Smith*, 2004]. Recent Mars general circulation model (MGCM) simulations have indicated that water ice clouds play an important role in the martian water cycle [*Richardson et al*. 2002; *Montmessin et al*. 2004; *Feldman et al.* 2005]. Simulations suggest that the tropical cloud belt undergoes a significant diurnal cycle, with maximum opacity in the early morning hours [*Hinson and Wilson*, 2004; *Feldman et al*. 2005]. It is anticipated that water ice clouds will provide a sensitive constraint for simulations of the atmospheric circulation and particularly water vapor transport. To date, observations of water ice clouds have been necessarily limited to daytime, although observations have hinted at diurnal cloud variations [*Akabane et al*. 2002]. In particular, TES cloud opacity retrievals require a high thermal contrast against a hot surface (> 220 K) and so are only available for 2pm observations [*Smith* 2004]. Here we describe a method of mapping the distribution of nighttime clouds by identifying their radiative signature on retrieved surface brightness temperature.

We have used MGS TES surface temperatures, albedo and thermal inertia estimates to derive improved thermal inertia (TI) fields suitable for use in versions of the GFDL MGCM with resolutions from 5x6° to 2x2.4° (*Wilson et al*. this workshop) By construction, the newly fitted TI fields allows the MGCM to predict the observed morning and afternoon temperatures in seasons and locations where our assumptions of atmospheric opacity are well founded. Since opacity leads to an increase in morning (2am) temperature and a decrease in afternoon (2pm) temperature, differences between observed and simulated temperatures largely reflect the influence of dust and/or water ice clouds not accounted for in a given simulation. Dust has a minor influence on surface temperature in the aphelion season, allowing the influence of ice clouds to be isolated. We compare simulations with and without radiatively active water ice clouds to show that clouds can have a detectable influence on nighttime surface temperature The recent analysis of MOLA laser returns [*Neumann et al*. 2003; *Sun et al*. 2005] provides corroboration of this technique.

General circulation model: The GFDL MGCM simulates the circulation of the Martian atmosphere with a comprehensive set of physical parameterizations [*Wilson and Hamilton* 1996; *Hinson and Wilson* 2004]. These include parameterizations for radiative transfer associated with CO_2 gas and aerosols. The dust aerosol may be specified or can be allowed to evolve with the circulation. The water cycle is represented by surface ice and regolith water reservoirs, atmospheric transport and ice cloud formation [*Richardson and Wilson* 2002]. We use a 2-stream method to account for aerosol scattering and absorption when calculating shortwave and longwave radiative fluxes. The relevant optical properties (Q_{ext}, ω, and *g*) are all functions of wavelength, and aerosol composition and size. Cloud radiative properties in the IR are described by *Wolff and Clancy* [2003]. We include a calculation of the simulated T_7 and T_{23} brightness temperatures, which are the appropriate quantities to compare with the observed TES surface brightness temperature. The predicted ice clouds are optionally radiatively active [*Hinson and Wilson* 2004].

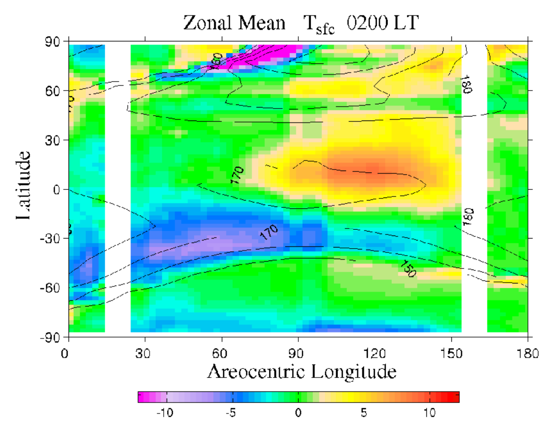

Figure 1. The seasonal evolution of zonally-averaged 2am surface temperature from a reference simulation employing a low (τ=0.15) atmospheric dust column is shown with 10 K contour intervals. The shading indicates the temperature anomaly defined by subtracting the reference field from the observed TES temperatures in MY25. A warm tropical temperature anomaly develops during the NH summer season.

Zonal mean surface temperatures: Figure 1 shows the seasonal evolution of zonally-averaged 2am surface temperature from a reference simulation representing relatively clear sky conditions. Also shown are the zonally-averaged differences between the observed and simulated surface temperatures. These differences emphasize the seasonal changes in observed temperatures that can be largely attributed to variations in atmospheric opacity. Daytime temperature differences [*Wilson et al*., this volume] are minimal during the relatively clear NH spring/summer season when the opacity assumed in the simulation most closely approximates that of the actual atmosphere. The figure reveals the development of warm tropical temperature anomaly in the solstice season that is strongly correlated with the waxing and waning of the tropical cloud belt evident in daytime ice opacity retrievals [*Smith* 2004]. Temperature differences in the vicinity of the retreating north polar cap are due, in part, to the influence of dust and ice clouds on retrieved brightness temperatures. We will show that the tropical temperature anomaly reflects the effect of enhanced IR warming by the nighttime tropical clouds.

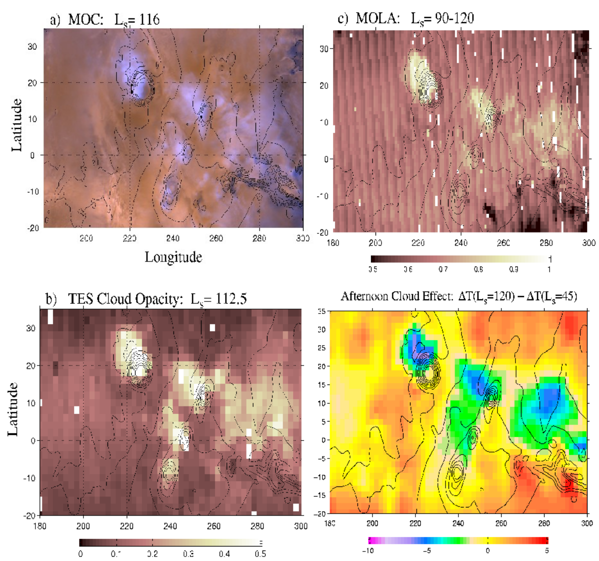

Figure 2. The spatial pattern of daytime (2pm) clouds in the Tharsis region during NH summer solstice as revealed by: (a) MOC imagery (b) Infrared opacity derived from TES spectra (c) absorption derived from MOLA and (d) inferred from surface temperature anomaly. Water ice clouds yield a negative temperature anomaly.

Daytime Clouds: Figure 2 shows the spatial distribution of daytime clouds in the Tharsis region as seen in MOC imagery (Fig. 2a) and derived from TES IR spectra (Fig. 2b), MOLA absorption (Fig. 2c) and TES surface temperatures by the method to be described below. The most prominent afternoon clouds tend to be localized downwind from the major volcanoes. The four panels provide a consistent view of the same reality. The seasonal variation of observed and simulated 2am and 2pm surface temperatures at two locations in the Tharsis region are shown in Figure 3. There are large perturbations in both daytime and nighttime temperatures due to dust storm activity in the perihelion season (L_s=180-350). However, it is striking that the observed 2am temperatures are anomalously warm during the NH summer solstice season when the atmosphere is most clear of dust aerosol.

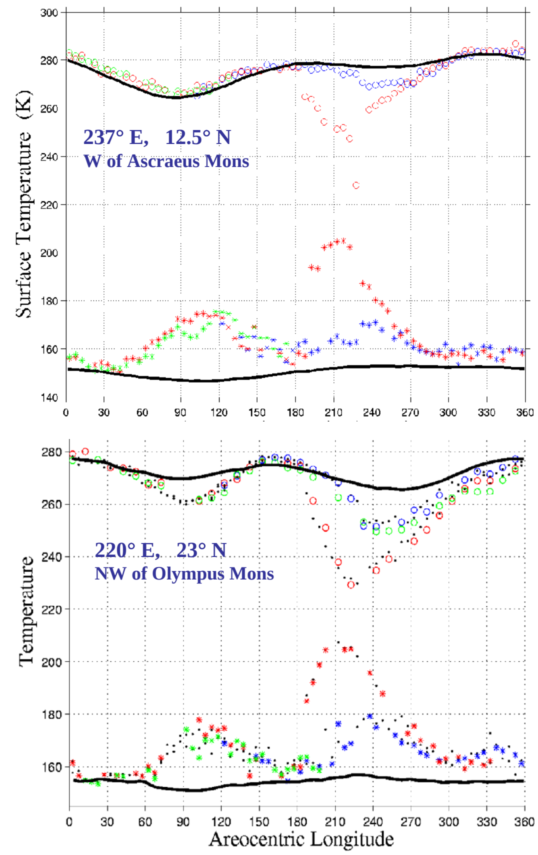

Figure 3. The seasonal variation of 2am (stars) and 2pm (circles) TES surface temperatures for two locations in the Tharsis region. Three Mars years are shown: MY24 (blue), MY25 (red), and MY26 (green). The solid curves represent the corresponding temperatures from the reference simulation. Differences between the reference and observed temperatures are largely due to the influence of dust and water ice clouds. The large nighttime temperature anomaly present around NH summer solstice is attributed to enhanced IR radiation from water ice clouds. The water ice cloud to the NW of Olympus Mons yields a clear daytime thermal signature.

Surface temperature anomaly fields (ΔT) can be constructed by subtracting the simulated reference temperature field from the observed TES surface temperatures. The influence of clouds can be isolated by differencing the NH solstice season anomaly field with an anomaly field of a period when clouds are less prominent. The MGCM simulation is in very close agreement with TES observations at L_s= 45° when the assumed low opacity (weak dust only) is most realistic. Differencing the two anomaly fields minimizes the influence of small biases resulting from errors in determining the best fit thermal inertia field used by the reference simulation. The result for daytime temperatures is shown in Fig. 2d. The correspondence with the other measures of daytime clouds is quite good, providing confidence in the technique. An analysis of MOLA absorption suggests that the cloud located on the NW flank of Olympus Mons has an optical depth of ~1.5 seen in Fig 3a. which is consistent with the opacity needed for simulations to yield the decline in temperature (T_7) of ~ 8K seen in Fig 3a.

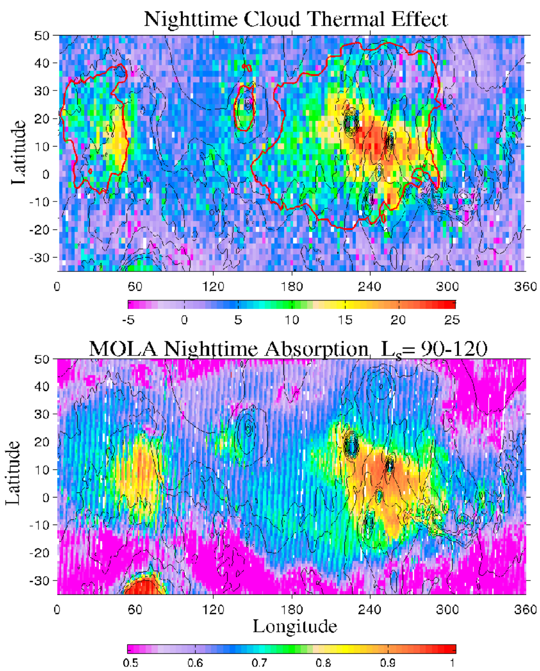

Figure 4. (a) Surface temperature anomaly field constructed by subtracting the simulated reference temperature field from observed TES nighttime surface temperatures for L_s= 110-120°. Red contours enclose regions of relatively low surface thermal inertia. (b) Nighttime MOLA absorption distribution.

Nighttime Clouds: The spatial pattern of the nighttime temperature anomaly is shown in Figure 4a. There is an enhanced temperature anomaly in the Tharsis region and a weaker and less extensive region in Arabia. This pattern is in close agreement with the pattern of high nighttime absorption revealed by MOLA in Figure 4b. This agreement strongly supports the interpretation of clouds being the source of the temperature anomaly. The Tharsis and Arabia regions are characterized by relatively low thermal inertia, and

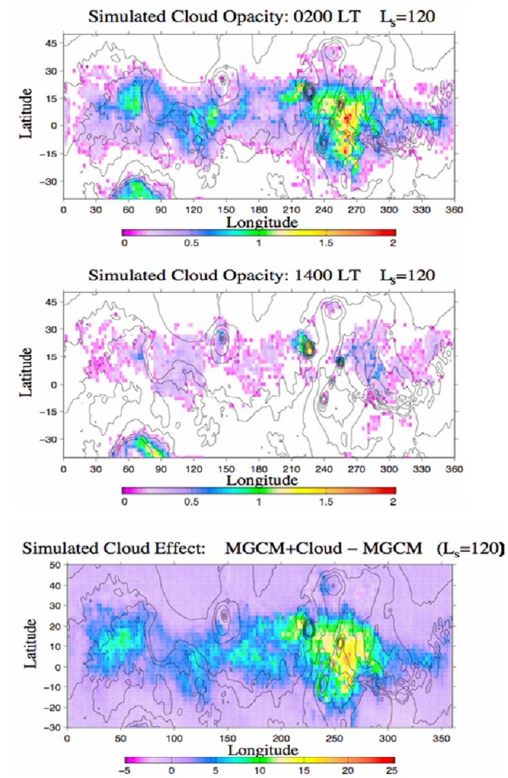

Figure 5. Simulated water ice cloud opacity for (a) nighttime and (b) daytime conditions. The simulation has a spatial resolution of 2°x2.4° and includes radiatively interactive water ice clouds (c) The simulated surface temperature anomaly is obtained by subtracting the reference surface temperature field from the corresponding surface temperatures from the simulation with radiatively active water ice clouds.

would be expected to have relatively strong response to enhanced IR radiation from nighttime clouds.

We carried out simulations with radiatively active water ice clouds to investigate the plausibility of clouds having the observed temperature effect. The simulatednighttime and daytime cloud opacities are shown in Figures 5a and 5b, respectively. The daytime opacity field is in good agreement with TES observations [*Smith*, 2004]. Inclusion of cloud radiation does yield an improved simulation. As suggested by the temperature anomaly map, the nighttime cloud field is considerably thicker and more extensive than the daytime cloud field. Figure 5c shows the increase in nighttime surface temperatures relative to the reference simulation which does not include cloud radiation. The simulation indicates that the enhanced downward infrared radiation from the simulated water ice clouds is able to reasonably account for the observed spatial pattern and amplitude of the surface temperature anomaly in Fig 4a. Additionally, the simulated cloud opacity of ~1.5 in Fig. 5a is consistent with the opacity

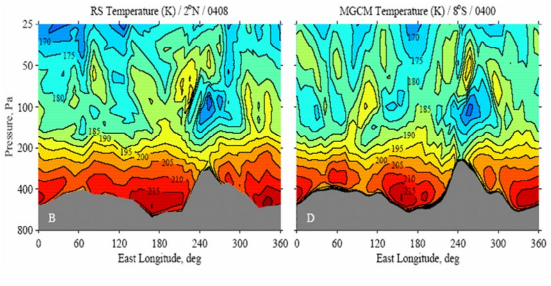

Figure 6. Longitude-height cross sections of temperature at fixed local time (0400 LT) derived from (a) RS measurements and (b) a MGCM simulation with radiatively active water ice clouds. RS and MGCM results are shown for L_s=145°. The contour interval is 5K and gray shading denotes the surface (From *Hinson and Wilson* [2004]).

needed to account for the peak absorptions seen by the MOLA instrument [*Sun et al*. 2005].

Figure 6a shows the presence of large amplitude temperature inversions in a longitudinal cross section of early morning (0400 LT) tropical temperature derived from Radio Science occultation data [*Hinson and Wilson*, 2004]. Significantly, simulated nighttime water ice clouds also provide sufficient radiative cooling to explain the temperature inversion in the Tharsis region. The downward propagation of the coupled cloud and temperature structure seen in Figure 7 is consistent with the amplification of the topographically-modulated diurnal tide by radiative heating/cooling associated with the tropical water ice clouds. By early morning, the simulated cloud has a relatively shallow structure, which is consistent with the interpretation of Hubble imagery of solstice season clouds by *Clancy et al*. [1996].

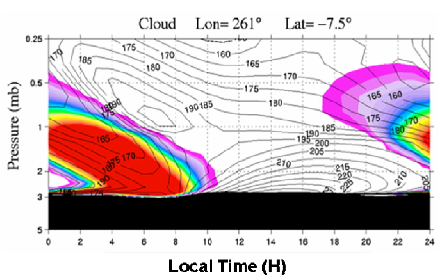

Figure 7. The diurnal evolution of the tropical ice cloud and temperature at a location within the Tharsis region. The cloud descends downwards in association with the diurnal thermal tide and is rapidly dissipated by daytime solar heating. In this season (L_s=145°), the tropical cloud belt has largely vanished from the afternoon observations. The pronounced temperature inversion at 0400 LT is consistent with the observations in Fig. 6a.

Discussion: Our indirect cloud retrievals are the first to spatially map the nighttime clouds and provide an estimate of their thermal influence. A comparison with the recent analysis of MOLA laser returns [*Neumann et al*. 2003; *Sun et al*. 2005] provides corroboration of the mapping of nighttime water ice clouds presented here. It appears that relatively thick nighttime water ice clouds (τ~1) can provide the enhanced IR radiation at the surface (greenhouse effect) needed to account for the observed temperature anomalies during the NH summer solstice season. It is likely that the radiative effects of water ice clouds have an influence on the zonal mean temperature distribution as well. Simulations suggest that the inclusion of cloud radiative heating/cooling leads to better agreement with the observed seasonal evolution of midlevel (0.5 mb) tropical temperatures. It is anticipated that radiative cooling by the polar hood clouds can have an effect on shaping the structure of the polar vortex during the spring and fall seasons. Simulations suggest that this can influence the properties of baroclinc waves embedded in the polar vortex.

References:

Akabane, T., T. Nakakushi, K. Iwasaki and S. M. Larson, Diurnal variation of Martian water-ice clouds in Tharsis region of the low latitude cloud belt: Observations in 1995-1999 apparitions, *Astron. Astrophys., 384*(2), 678-688, 2002.

Clancy, R.T., *et al*., Water vapor saturation at low altitudes around Mars aphelion: A key to Mars climate*?, Icarus, 122*, 36-62, 1996.

Feldman, W.C., *et al*. Topographic control of hydrogen deposits at low latitudes to midlatitudes of Mars, *J. Geophys. Res., 110*, 2005.

Hinson, D., and R.J. Wilson, Temperature inversions, thermal tides, and water ice clouds in the Martian tropics, *J. Geophys. Res., 109, E01002*, 2004.

Montmessin, F., F. Forget, P. Rannou, M. Cabane, and R.M. Haberle, Origin and role of water ice clouds in the martian water cycle as inferred from a general circulation model, *J. Geophys. Res*., *109*, E10004, 2004.

Neumann, G. A.; D.E. Smith, and M. T. Zuber, Two Mars years of clouds detected by the Mars Orbiter Laser Altimeter, *J. Geophys. Res*., *108 (E4)*, 10.1029/2002JE001849, 2003.

Richardson, M.I., and R.J. Wilson, Investigation of the nature and stability of the martian seasonal water cycle with a general circulation model, *J. Geophys. Res*., *107*(E5), 2002.

Smith, M.D., Interannual variability in TES Atmospheric observations of Mars during 1999-2003, *Icarus, 108*, 148-165, 2004.

Sun, X., G.A. Neumann, J.B. Abshire, and M.T. Zuber, Mars 1064-nm spectral radiance measurements from the receiver noise response of the Mars Orbiter Laser Altimeter, *Applied Optics*, in press, 2005.

Wilson, R.J., and K.P. Hamilton, Comprehensive model simulation of thermal tides in the Martian atmosphere, *J. Atmos. Sci*., *53*, 1290-1326, 1996

Wolff, M.J., and R.T. Clancy, Constraints on the size of Martian aerosols from Thermal Emission Spectrometer observations, 2003.